Applied Radiation and Isotopes 184 (2022) 110122

Contents lists available at ScienceDirect

Applied Radiation and Isotopes

journal homepage: www.elsevier.com/locate/apradiso

# Experimental determination of $k_0$ and $Q_0$ values for $^{121}$Sb, $^{123}$Sb and $^{130}$Ba targets applying covariance analysis

L.F. Barros *, M.S. Dias, M.F. Koskinas

*Instituto de Pesquisas Energéticas e Nucleares (IPEN-CNEN/SP), Centro do Reator de Pesquisas - CRPq, C.P. 11049, Pinheiros, 05422-970, São Paulo, SP, Brazil*

ARTICLE INFO

*Keywords:*
$k_0$ method
Gamma-ray spectrometry
Ba Sb Isotopes
Neutron activation analysis
Nuclear reactor

ABSTRACT

This work consists of an experimental determination of $k_0$ and $Q_0$ for $^{121}$Sb, $^{123}$Sb and $^{130}$Ba targets. Covariance analysis has been introduced to supply not only the overall uncertainties in these parameters but also their correlations. The irradiations were performed near the core of the IEA-R1 4.5 MW swimming-pool nuclear research reactor of the Nuclear and Energy Research Institute (IPEN-CNEN/SP), in São Paulo, Brazil. The epithermal neutron flux shape parameter, alpha, at the irradiation position is very close to zero, which favors to obtain $Q_0$ values more accurately. Two irradiations were carried out in sequence, using two sets of samples: the first with bare samples and the second inside a Cd cover. The activity measurements were carried out in a previously calibrated HPGe gamma-ray spectrometer. The measurements were corrected for: saturation, decay time, cascade summing, geometry, self-attenuation, measuring time and mass. Standard sources of $^{152}$Eu, $^{133}$Ba, $^{60}$Co and $^{137}$Cs traceable to a 4πβ−γ primary system were used to obtain the HPGe gamma-ray peak efficiency as a function of the energy. The experimental efficiency curve was performed by a fourth-degree polynomial fit, in the energy range of the standard sources, 121–1408 keV, it contains all correlations between points. For energies above 1408 keV, the efficiencies were obtained by the Monte Carlo Method. The covariance matrix methodology was applied to all uncertainties involved. The final values for $k_0$ and $Q_0$ were compared with the literature.

## 1. Introduction

The $k_0$ standardization method has grown from a mere theoretical concept to a fully operational tool (De Corte, 1987). The nuclear parameters $k_0$ and $Q_0$ have been experimentally determined by several laboratories around the world (Farina Arboccò et al., 2014; Barros et al., 2019; Chilian et al., 2014; Jaćimović et al., 2014; Lin and Von Gostomski, 2013; Stopic and Bennett, 2014; Li et al., 2021). This has been done to refine the values of these nuclear constants, adding new data to the Nuclear Data Sub-Committee $k_0$ Database (Jaćimović, 2020).

In the present study, the $k_0$ and $Q_0$ parameters were determined for $^{121}$Sb, $^{123}$Sb and $^{130}$Ba targets, corresponding to the neutron capture reactions $^{121}$Sb(n, γ) $^{122}$Sb, $^{123}$Sb(n, γ) $^{124}$Sb and $^{130}$Ba(n, γ) $^{131}$Ba, respectively. The covariance matrix methodology has been applied in order to supply not only the overall uncertainties in these parameters but also their correlations (Barros, 2018; Barros et al., 2019; Dias et al., 2010, 2011).

The $k_0$ and $Q_0$ determination for the $^{130}$Ba(n, γ) $^{131}$Ba reaction has historical problems described at the Second Research Coordination Meeting on Reference Database for Neutron Activation Analysis (Firestone and Kellett, 2008), by Kennedy's list of suspicious $k_0$ values, published by the IAEA Nuclear Data Section (Kellett, 2009), by Lin et al. (2007), De Corte (2010) and Farina Arboccò (2017).

Different $Q_0$ values for the $^{121}$Sb(n,γ) $^{122}$Sb and $^{123}$Sb(n,γ)$^{124}$Sb reactions have been reported by De Corte and Simonits (2003), Farina Arboccò et al. (2014) and Mughabghab, cited by Trkov (2002). Discrepancies in the $k_0$ and $Q_0$ values for $^{121}$Sb(n,γ) $^{122}$Sb and $^{123}$Sb(n, γ)$^{124}$Sb reactions were also addressed at the First Research Coordination Meeting on Reference Database for Neutron Activation Analysis (Firestone and Trkov, 2005).

The irradiations were conducted at position 24A, near the core of the IEA-R1 4.5 MW swimming-pool nuclear research reactor of the Instituto de Pesquisas Energéticas e Nucleares (IPEN-CNEN/SP – Nuclear and Energy Research Institute), in São Paulo, Brazil.

The thermal neutron flux of IEA-R1 was 2.63 (4) × $10^{13}$ cm$^{-2}$ s$^{-1}$. The neutron spectrum shape parameter $\alpha$ is very close to zero at this irradiation position and, as a result, the correction to be applied for the determination of $Q_0$ is very close to one. As expected, previous works

* Corresponding author.,
*E-mail addresses:* lfbarros@ipen.br, msdias@ipen.br (L.F. Barros).

https://doi.org/10.1016/j.apradiso.2022.110122
Received 15 July 2021; Received in revised form 8 November 2021; Accepted 20 January 2022
Available online 23 January 2022

performed at the same irradiation position provided $Q_0$ results with good accuracy (Barros et al., 2019; Dias et al., 2010, 2011).

For each experiment, two irradiations were carried out in sequence: the first with bare samples and the second with a cadmium cover around the samples. Each sample was irradiated together with an Al–Au (0.1%) alloy wire, on each side, used as comparator. All partial uncertainties were considered, applying the covariance matrix methodology.

## 2. Materials and methods

In the present work all $k_0$ and $Q_0$ factors were determined with Au as comparator ($^{197}$Au(n,γ)$^{198}$Au, $E_\gamma$ = 411.8 keV). For $k_0$ determination, the measurements were carried out at 18.97 cm sample-detector distance. This distance was chosen for the purpose of reducing the cascade sum correction. The sources were positioned in a lucite support that provides 18.97 cm away from the crystal front face.

The $k_0$ factor for each energy of the gamma radiation of the $^{121}$Sb (n,γ)$^{122}$Sb and $^{123}$Sb(n,γ)$^{124}$Sb reactions was obtained by the weighted average with covariance of the $k_0$ values determined by two methods: the *Cd-subtraction method* ($k_{01}$) and the *Bare sample method* ($k_{02}$), described by De Corte (1987).

The $k_0$ factor for each $^{131}$Ba gamma-ray energy obtained from $^{130}$Ba (n,γ)$^{131}$Ba reaction was obtained only by the *Bare sample method* (De Corte, 1987). The *Cd-subtraction method* was not feasible due to very low sample counting rates of the samples under Cd cover.

The neutron spectrum shape parameter $\alpha$ for the irradiation position was obtained previously (Barros et al., 2019), by the weighted average of the $\alpha$ values acquired by the *Cd-covered multi-monitor method* and by the *Cd-ratio multi-monitor method* (De Corte, 1987).

The parameter *f*, which corresponds to the ratio between the thermal and epithermal neutron fluxes, was determined by the *Cd-ratio multi-monitor method* (De Corte, 1987).

For $Q_0$ determination of $^{121}$Sb(n, γ)$^{122}$Sb and $^{123}$Sb(n, γ)$^{124}$Sb reactions, the measurements were carried out at 18.97 cm sample-detector distance. For $Q_0$ determination of the $^{130}$Ba(n, γ) $^{131}$Ba reaction, the measurements at a closer distance, 2.29 cm, were necessary to evaluate the results for the most intense gamma-ray energy: 496.33 keV (47%) due to low counting rates at longer distances for the Cd covered samples.

The $Q_0$ value for the $^{121}$Sb(n, γ) $^{122}$Sb, $^{123}$Sb(n, γ) $^{124}$Sb and $^{130}$Ba(n, γ) $^{131}$Ba reactions was calculated from $Q_0$ ($\alpha$) by the expressions mentioned by De Corte (1987). The $Q_0$ factor was obtained by the weighted average of $Q_0$ values of all gamma-ray transitions for each corresponding reaction. For $k_0$ and $Q_0$ determination, the pairs of Ba and antimony Sb, with and without cadmium cover, were combined with the closest Au–Al wires.

The values of effective resonance energy $\overline{E}_{r,i}$ were taken from (Jaćimović, 2020). The values of self-shielding correction factors $G_{th}$ and $G_e$, calculated by code MATSSF (Trkov, 2016), were close to one because the samples were embedded in filter paper, as described in the following section.

### 2.1. Sample preparation and irradiation

The samples were taken from certified solutions (*VHG Labs*) and embedded in filter papers, previously to the irradiation. Alloys of Au (0.10% in Al, IRMM–530RC) were used as monitors during the irradiations. All masses were measured accurately by a Mettler Toledo XP56 microbalance and the samples were placed in the irradiation position 24A, near the 4.5 MW IEA-R1 reactor core. The samples were wrapped with thin aluminum foils and positioned in the middle of a cylindrical aluminum container (*rabbit*) 7.0 cm long, 2.1 cm in diameter and 0.05 cm thick. To compensate for the neutron flux gradient along the distance from the rabbit axis, positioned parallel to the reactor core, each sample was sandwiched within a pair of Au samples. They were irradiated in duplicate, one at each side of a rectangular aluminum sheet used to mount them inside the *rabbit*. In this way, three Au–Al samples were irradiated together with two target samples in each *rabbit*. Two sets of *rabbits* were prepared for each experiment: one with a cadmium cover around the samples and the other without it. These sets were irradiated during 60 min each, in sequence: the first without cadmium cover and the second with it. Inside the *rabbits* that stored the barium samples, the samples named Ba2, Ba4, Au–Al2, Au–Al4 and Au–Al6 were irradiated without cadmium cover, and the samples Ba1, Ba3, Au–Al1, Au–Al3 and Au–Al5 were irradiated with a cadmium cover, as shown in Fig. 1. The preparation of the antimony samples inside the *rabbits* followed the same procedure, also described in a previous work (Barros et al., 2019). The irradiations of the barium and antimony samples were performed in November and December 2019, respectively. The minimum decay time before measurements was around 24 h.

### 2.2. Efficiency calibration

Standard sources of $^{60}$Co, $^{133}$Ba, $^{137}$Cs and $^{152}$Eu, traceable to the LMN 4πβ−γ absolute system, were used for obtaining the HPGe gamma-ray peak efficiency as a function of the energy. These sources were positioned 18.97 cm away from the crystal front face. An accurate pulser was introduced in the gamma-ray spectrum close to the right edge, to perform dead time and pile-up corrections.

A fourth-degree polynomial in log-log scale was fitted between the HPGe peak efficiency and the normalized gamma-ray energy $E/E_0$, where $E_0$ is an arbitrary energy (800 keV), chosen to reduce the uncertainty in the interpolation (Dias et al., 2004) and covering the 121 keV–1408 keV energy range. This least square fitting was performed by code LOGFIT V.1 (Dias and Moreira, 2005), developed by the Nuclear Metrology Laboratory (LMN - Laboratório de Metrologia Nuclear), at the IPEN-CNEN/SP. The efficiency curve was complemented by Monte Carlo calculations applying code MCNP6 with optimized source-detector dimensions. For energies greater than 1408 keV were considered the efficiencies obtained by the Monte Carlo Method.

The results of efficiency ratios between the comparator (Au) and the target reaction products, comparing the fitted efficiency by the Polynomial (experimental efficiency curve) and the calculated efficiencies by Monte Carlo in the energy interval of 121–1408 keV, indicated a good agreement, with an average difference of 1.06%. Considering this result, the experimental efficiency curve was adopted in this energy interval as it contains all correlations between points.

### 2.3. Cascade summing correction

The cascade summing corrections were calculated by NUCSUM code, version 8.0, which is a part of the SUMCOR code package developed by the LMN (Dias et al., 2018). The procedure to calculate the cascade summing correction is based on the Semkow formalism (Semkow et al., 1990). The determination of cascade summing corrections was succeeded based on MCNP6 modelling.

### 2.4. Gamma-ray spectrometry measurements

The number of counts observed by the HPGe detector for the gamma-ray transitions of $^{122}$Sb, $^{124}$Sb e $^{198}$Au were evaluated using the ALPINO V.1 (Dias and ALPINO, 2001). The ALPINO V.1 was developed by LMN in FORTRAN language; the program calculates efficiency or activity; area under the peak of total absorption, dead time correction, it has the option to subtract the background counts, it marks the limit of the channels where the peak is, it determines the Full Width at Half Maximum (FWHM) and it allows the user to enter arbitrary choice of channels to calculate the peak area. This code was used to evaluate the number of counts in these cases because there were no overlapped peaks in the analyzed spectra.

On the other hand, the photopeaks of interest for $^{131}$Ba at 246 and 249 keV overlap. In this case the net peak area was evaluated using the

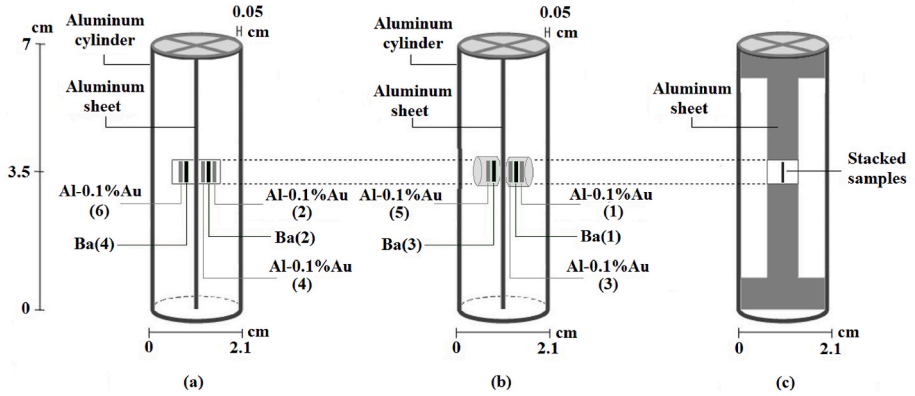


**Fig. 1.** Rabbits prepared for the irradiations with Au–Al and Ba samples; (a) Samples without cadmium cover; (b) Samples with cadmium cover; (c) Rabbit front view. The numbers inside parentheses correspond to the sample identification. Similar rabbits were prepared for Sb and Au–Al samples.

Hypermet 5.12 analysis software (Hypermet, 2008). Even very complicated multiplets can be successfully and automatically resolved with minimal user interaction by this software.

For the $k_0$ factor determination, the irradiated barium and antimony samples were measured at 18.97 cm sample-detector distance. For the $Q_0$ factor determination of $^{130}Ba(n,\gamma)^{131}Ba$ reaction, the irradiated samples were measured at 2.29 cm sample-detector distance, and evaluated at its most intense gamma emission energy of 496.33 keV (Iγ of 47%). For the $Q_0$ factors determination of the $^{121}Sb(n,\gamma)^{122}Sb$ and $^{123}Sb(n,\gamma)^{124}Sb$ reactions, the irradiated samples were measured at 18.97 cm sample-detector distance.

### 2.5. Covariance matrix methodology

The discussion on the covariance methodology applied to the conventional formalism has already been presented in our previous papers (Dias et al., 2010, 2011). This methodology employs the use of the Covariance Matrix for the calculation of uncertainties, which is essential for a complete description of the partial uncertainties involved. This matrix contains the variance of each of the parameters and the covariance between each pair of parameters. All partial uncertainties involved were identified and the degree of dependence among all parameters involved in the parameters $k_0$ and $Q_0$ was determined. The COVAR V.4.2 program was developed by the LMN (Nuclear Metrology Laboratory) with the purpose of determining the covariance between the $k_0$ values, calculated by the two methods: the *Cd-subtraction method* ($k_{01}$) and the *Bare sample method* ($k_{02}$), and the $Q_0$ values.

## 3. Results and discussion

The behavior of the peak efficiency as a function of the gamma-ray energy for the HPGe spectrometer, conducted in 2019 is presented in Fig. 2. The results indicated in black and gray marks correspond to experimental and theoretical efficiencies calculated by MCNP6, respectively. The continuous line corresponds to a 4th degree polynomial fit in log-log scale. The coefficients $a_0$, $a_1$, $a_2$, $a_3$, $a_4$, their absolute uncertainties and its Correlation Matrix are shown in Table 1. The reduced Chi-Square value was 1.50 indicating a reasonable fit.

The values obtained for experimental efficiency, fitted by the 4th degree polynomial, and theoretical efficiency, calculated by MCNP6, for respective energies of the target reaction products, $^{131}Ba$, $^{122}Sb$ and $^{124}Sb$, the efficiency ratio between the comparator (Au) and the target reaction products determined by MCNP6 and by the fitted polynomial, as well as the percentage differences of these values are presented in Table 2.

The self-shielding correction factor for thermal and epithermal neutrons, $G_{th}$ and $G_e$, respectively, and the cadmium transmission factor

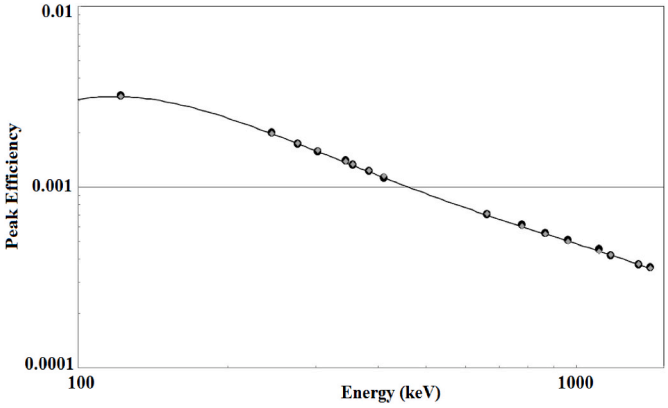


**Fig. 2.** HPGe peak efficiency as a function of the gamma-ray energy. The black and gray marks correspond to the experimental and theoretical efficiencies calculated by MCNP6, respectively, in the energies of the standard sources. The energy interval of the standard sources is 121–1408 keV.

**Table 1**
Parameters and Correlation Matrix of the efficiency curve fitting. The fitted function was: $ln(\varepsilon) = a_0 + a_1[ln(E/E_0)] + a_2[ln(E/E_0)]^2 + a_3[ln(E/E_0)]^3 + a_4[ln(E/E_0)]^4$ and $E_0 = 800$ keV.

| Parameter | | Absolute Uncertainty | Correlation Matrix ( × 1000) |
|---|---|---|---|
| $a_0$ | −7.43 | $6.7 \times 10^{-3}$ | 1000 |
| $a_1$ | $-8.79 \times 10^{-1}$ | $1.2 \times 10^{-2}$ | −87 1000 |
| $a_2$ | $7.84 \times 10^{-2}$ | $1.3 \times 10^{-2}$ | −420 -107 1000 |
| $a_3$ | $-1.58 \times 10^{-1}$ | $2.8 \times 10^{-2}$ | −109 -848 505 1000 |
| $a_4$ | $-1.04 \times 10^{-1}$ | $1.2 \times 10^{-2}$ | −28 -881 325 978 1000 |
| $\chi^2/\nu$ | 1.50 | | |

$F_{Cd}$ of the $^{121}Sb$, $^{123}Sb$, $^{130}Ba$ and $^{197}Au$ are shown in Table 3.

The value of $\alpha$ used in this work was $-4.9\ (59) \times 10^{-3}$, according to Barros et al. (2019). This value is close to zero, indicating an epithermal neutron field approaching the ideal spectrum. The $f$ values calculated in this work, from the Au–Al monitors irradiated with the barium and antimony samples were 45.8 (12) and 46.3 (12), respectively. The numbers inside parentheses are the uncertainties in the last digits (one standard deviation).

At the 18.97 cm sample-detector distance, the cascade summing correction for the energies of the standard sources of $^{60}Co$, $^{133}Ba$, $^{137}Cs$ and $^{152}Eu$, traceable to a $4\pi\beta-\gamma$ primary system, was below 0.94%, with an uncertainty of less than 0.2%, and, for the energies of $^{122}Sb$, $^{124}Sb$ e $^{131}Ba$, it was below 7%, with an uncertainty less than 1.5%.

The $k_0$ results for the conventional methods A ($k_{01}$) and B ($k_{02}$), the $k_0$

**Table 2**
Values obtained for experimental efficiency, fitted by the polynomial, and theoretical efficiency, calculated by MCNP6, for respective energies of the target reaction products, the efficiency ratio between the comparator (Au) and the target reaction products determined by MCNP6 and by the fitted polynomial, and the percentage differences of these values. The numbers inside parentheses are the uncertainties in the last digits (one standard deviation).

| | Target reaction product | Gamma Energy (keV) | Efficiency by *Monte Carlo Method* ( $\times 10^{-3}$) | Fitted Efficiency by the Polynomial ( $\times 10^{-3}$) | Dif. (%) | Ratio [Target efficiency ($\varepsilon_{p,i}$) /Au efficiency ($\varepsilon_{p,Au}$) | | Dif. (%) |
|---|---|---|---|---|---|---|---|---|
| | | | | | | *Monte Carlo Method* | Fitted Efficiency by the Polynomial | |
| | $^{131}$Ba | 123.8 | 3.162 (34) | 3.165 (30) | −0.09 | 2.752 (42) | 2.813 (34) | −2.16 |
| | | 133.6 | 3.072 (33) | 3.115 (30) | −1.38 | 2.674 (41) | 2.768 (34) | −3.42 |
| | | 216.1 | 2.239 (24) | 2.242 (22) | −0.13 | 1.949 (30) | 1.992 (25) | −2.20 |
| | | 239.6 | 2.029 (22) | 2.022 (18) | 0.35 | 1.766 (27) | 1.797 (21) | −1.72 |
| | | 249.4 | 1.952 (21) | 1.940 (17) | 0.62 | 1.699 (26) | 1.724 (20) | −1.48 |
| | | 373.2 | 1.274 (14) | 1.251 (9) | 1.84 | 1.109 (17) | 1.112 (12) | −0.29 |
| | | 404.0 | 1.171 (13) | 1.149 (8) | 1.91 | 1.019 (16) | 1.021 (10) | −0.17 |
| | | 486.5 | 0.966 (10) | 0.9450 (72) | 2.22 | 0.841 (13) | 0.8398 (90) | 0.12 |
| | | 496.3 | 0.948 (10) | 0.9259 (70) | 2.39 | 0.825 (13) | 0.8228 (87) | 0.23 |
| | | 585.0 | 0.8006 (87) | 0.7869 (58) | 1.74 | 0.697 (11) | 0.6993 (73) | −0.36 |
| | | 620.1 | 0.7566 (82) | 0.7445 (53) | 1.63 | 0.658 (10) | 0.6616 (68) | −0.47 |
| | | 1047.6 | 0.4640 (50) | 0.4671 (31) | −0.66 | 0.404 (6) | 0.4151 (41) | −2.71 |
| | $^{122}$Sb | 564.2 | 0.8300 (90) | 0.8151 (61) | 1.83 | 0.722 (11) | 0.7243 (77) | −0.27 |
| | $^{124}$Sb | 692.7 | 0.6792 (74) | 0.6718 (46) | 1.10 | 0.591 (9) | 0.5970 (60) | −0.98 |
| | | 602.7 | 0.7785 (84) | 0.7648 (56) | 1.79 | 0.678 (10) | 0.6796 (71) | −0.31 |
| | | 645.9 | 0.7266 (79) | 0.7166 (51) | 1.40 | 0.632 (30) | 0.6368 (66) | −0.70 |
| | | 722.8 | 0.6526 (71) | 0.6466 (45) | 0.93 | 0.568 (9) | 0.5746 (59) | −1.15 |
| | | 1691.0 | 0.2981 (32) | – | – | 0.259 (4) | – | – |
| | | 2090.9 | 0.2422 (26) | – | – | 0.211 (3) | – | – |
| | $^{198}$Au | 411.8 | 1.149 (12) | 1.1253 (84) | 2.11 | – | – | – |
| **Average** | | | | | **1.08** | | | **−1.06** |
| **Standard deviation from the mean** | | | | | **1.08** | | | **0.87** |

**Table 3**
Values obtained for $G_{th}$, $G_e$ and $F_{Cd}$; the numbers inside parentheses are the uncertainties in the last digits (one standard deviation).

| Target | $G_{th}$ | $G_e$ | $F_{Cd}$ [a] |
|---|---|---|---|
| $^{121}$Sb | 1.0000 | 1.0000 | 0.992(1) |
| $^{130}$Ba | 1.0000 | 1.0000 | 0.998(1) |
| $^{197}$Au | 1.0000 | 1.0000 | 0.998(1) |
| $^{123}$Sb | 0.9990(2) | 0.9956(9) | 0.991(1) |

[a] Trkov et al., 2015.

factor and the Zeta Score factor between pairs of $k_0$ values, obtained in this work and compared with the literature, are presented in Table 4. The $Q_0$ factor and the Zeta Score factor between values obtained in this work and from the literature are presented in Table 5. The Zeta Score factor is defined by ISO 13528 (2015). Agreement was considered when the absolute value of this factor was below 3.0 (99% confidence interval). The number inside parentheses corresponds to the uncertainty in the last digits (one standard deviation). There is a good agreement among the three methods within the corresponding uncertainties. The $k_0$ factor for the $^{122}$Sb and $^{124}$Sb was obtained by the weighted average of the methods A ($k_{01}$) and B ($k_{02}$), considering the correlations between the methods.

For $^{121}$Sb(n,γ)$^{122}$Sb and $^{123}$Sb(n,γ)$^{124}$Sb reactions, the $k_0$ values given by De Corte and Simonits (2003) and Jaćimović (2020) are the same for all energies considered in this work. The $k_{01}$ values agree well with $k_{02}$ values for all considered energies, within the corresponding uncertainties. For $^{122}$Sb and $^{124}$Sb, the $k_0$ factors obtained in this work agree with De Corte and Simonits (2003) and Jaćimović (2020) for all considered energies.

The $k_0$ factor obtained in this work for the energy of 564.2 keV of the $^{122}$Sb does not agree with the value from Farina Arboccò et al. (2014). The $k_0$ factors obtained for the energies of 602.73 and 645.85 keV of the $^{124}$Sb agree marginally with the values from Farina Arboccò et al. (2014).

The $k_0$ factors from the present work for the energy of 692.7 keV of the $^{122}$Sb and for the energies of 722.78, 1690.97 and 2090.95 keV of the $^{124}$Sb agree with the values of Farina Arboccò et al. (2014).

It was observed in the evaluated spectra of the $^{131}$Ba samples the presence of the gamma emission peak of 246.885 keV (Iγ of 0.632%). As the error of the area under the peak of total absorption in the energy of 246.885 keV was a very high value, around 30%, the parameter $k_0$ for this energy was not considered in this work. In addition, an overlap of this peak of 246.885 keV was observed with the peak of 249.432 keV (Iγ of 2.813%), so the areas under the overlapping peaks at these two energies were evaluated by code Hypermet 5.12, which performs the deconvolution of the photopeaks. The $k_0$ factor that has not yet been evaluated in the current literature for $^{131}$Ba in this energy region, therefore it was inserted at the energy of 248.96 keV, which is the weighted average between 246.885 and 249.432 keV considering their gamma emission intensities (Iγ of 0.632% and 2.813%, respectively), which is a new value of $k_0$ to be included in the literature.

The $k_0$ factors obtained in this work for the reaction $^{130}$Ba(n,γ) $^{131}$Ba agree with the values of the Jaćimović (2020) in the energies of 123.81; 133.61; 216.08; 239.63; 249.43; 404.05; 486.52; 496.33; 620.11 and 1047.60 keV and they marginally agree at the energy of 373.25 keV. The values from the present work agree with the values of De Corte and Simonits (2003) in the energies of 123.81; 373.25 and 496.33 keV and they agree marginally in the energy of 216.08 keV. They agree with the values of X. Lin and Von Gostomski (2013) in the energies of 123.81; 216.08 and 496.33 keV and agree marginally at the energy of 373.25 keV.

A difference of 28% was observed between the $k_0$ value of the present work, for the gamma-ray energy of 239.63 keV from the $^{130}$Ba(n,γ) $^{131}$Ba reaction, with the only one value found in the literature, the $k_0$ value of Jaćimović (2020), showing a zeta score of 2.59 between them. The fact that there is only one value in the literature for this energy limits the comparison. The subtraction of $^{232}$Th– $^{212}$Pb background peak of energy 238.63 keV was considered in the spectrum analysis in order to obtain this $k_0$ value.

**Table 4**
Results obtained for $k_0$ by different methods. Method *A* corresponds to the *"Cd-subtraction method";* Method *B* corresponds to the *"Bare sample method"*. There is a comparison between the $k_0$ values obtained in this work and from the literature applying the Zeta score parameter. Agreement was considered for Zeta below 3.0 (99% confidence interval). The numbers inside parentheses correspond to uncertainties in the last digits (one standard deviation). The references are indicated by a superscript and are described at the bottom of the table.

| Reaction | Gamma Energy (keV) | Method A ($k_{01}$) | Method B ($k_{02}$) | $k_0$ | Literature (indicated as superscript) | | | Zeta Score factor between pairsof $k_0$ values | | |
|---|---|---|---|---|---|---|---|---|---|---|
| $^{121}$Sb (n.γ)$^{122}$Sb | 564.2 | 4.47(9) × $10^{-2}$ | 4.43(10) × $10^{-2}$ | 4.45(10) × $10^{-2}$ | 4.38(7) × $10^{-2}$ a, b | | 4.00(8) × $10^{-2}$ c | 0.59 a,b | | 3.47 c |
| | 692.7 | 2.35(5) × $10^{-3}$ | 2.33(5) × $10^{-3}$ | 2.34(5) × $10^{-3}$ | 2.38(5) × $10^{-3}$ a, b | | 2.18(4) × $10^{-3}$ c | −0.52 a, b | | 2.45 c |
| $^{123}$Sb (n.γ)$^{124}$Sb | 602.73 | 3.03(5) × $10^{-2}$ | 3.01(6) × $10^{-2}$ | 3.02(6) × $10^{-2}$ | 2.96(2) × $10^{-2}$ a, b | | 2.80(5) × $10^{-2}$ c | 1.02 a,b | | 2.88 c |
| | 645.85 | 2.26(3) × $10^{-3}$ | 2.25(4) × $10^{-3}$ | 2.25(4) × $10^{-3}$ | 2.21(2) × $10^{-3}$ a, b | | 2.11(4) × $10^{-3}$ c | 1.08 a, b | | 2.70 c |
| | 722.78 | 3.27(6) × $10^{-3}$ | 3.25(7) × $10^{-3}$ | 3.26(7) × $10^{-3}$ | 3.19(3) × $10^{-3}$ a, b | | 3.08(5) × $10^{-3}$ c | 0.96 a,b | | 2.08 c |
| | 1690.97 | 1.44(3) × $10^{-2}$ | 1.43(3) × $10^{-2}$ | 1.43(3) × $10^{-2}$ | 1.41(2) × $10^{-2}$ a, b | | 1.38(2) × $10^{-2}$ c | 0.70 a, b | | 1.40 c |
| | 2090.95 | 1.66(3) × $10^{-3}$ | 1.65(3) × $10^{-3}$ | 1.65(3) × $10^{-3}$ | 1.58(3) × $10^{-3}$ a, b | | 1.58(3) × $10^{-3}$ c | 1.65 a, b | | 1.74 c |
| $^{130}$Ba (n.γ)$^{131}$Ba | 123.81 | | 3.56(13) × $10^{-5}$ | 3.56(13) × $10^{-5}$ | 3.78(6) × $10^{-5}$ a | 3.90(3) × $10^{-5}$ b | 3.657(8) × $10^{-5}$ d | −1.51 a | −2.58 b | −0.61 d |
| | 133.61 | | 2.74(12) × $10^{-6}$ | 2.74(12) × $10^{-6}$ | 2.97(30) × $10^{-6}$ a | 3.24 × $10^{-6}$ b | | −0.72 a | | |
| | 216.08 | | 2.61(4) × $10^{-5}$ | 2.61(4) × $10^{-5}$ | 2.60(4) × $10^{-5}$ a | 2.75(4) × $10^{-5}$ b | 2.520(6) × $10^{-5}$ d | 0.12 a | −2.72 b | 1.27 d |
| | 239.63 | | 4.13(13) × $10^{-6}$ | 4.13(13) × $10^{-6}$ | 3.23(32) × $10^{-6}$ a | | | 2.59 a | | |
| | 248.96 | | 3.89(49) × $10^{-6}$ | 3.89(49) × $10^{-6}$ | n.r. a | n.r. b | n.r. d | | | |
| | 249.43 | | 4.04(28) × $10^{-6}$ | 4.04(28) × $10^{-6}$ | 3.69(37) × $10^{-6}$ a | | | 0.76 a | | |
| | 373.25 | | 1.94(3) × $10^{-5}$ | 1.94(3) × $10^{-5}$ | 1.83(2) × $10^{-5}$ a | 1.920(8) × $10^{-5}$ b | 1.801(4) × $10^{-5}$ d | 2.79 a | 0.54 b | 2.62 d |
| | 404.05 | | 1.90(18) × $10^{-6}$ | 1.90(18) × $10^{-6}$ | 1.73(17) × $10^{-6}$ a | | | 0.67 a | | |
| | 486.52 | | 3.25(15) × $10^{-6}$ | 3.25(15) × $10^{-6}$ | 2.78(28) × $10^{-6}$ a | 3.44 × $10^{-6}$ b | | 1.48 a | | |
| | 496.33 | | 6.46(8) × $10^{-5}$ | 6.46(8) × $10^{-5}$ | 6.19(8) × $10^{-5}$ a | 6.48(1) × $10^{-5}$ b | 6.069(14) × $10^{-5}$ d | 2.37 a | −0.24 b | 2.43 d |
| | 620.11 | | 2.09(13) × $10^{-6}$ | 2.09(13) × $10^{-6}$ | 1.88(19) × $10^{-6}$ a | 2.34 × $10^{-6}$ b | | 0.92 a | | |
| | 1047.60 | | 1.72(16) × $10^{-6}$ | 1.72(16) × $10^{-6}$ | 1.72(17) × $10^{-6}$ a | | | −0.02 a | | |

The numbers inside parentheses are the uncertainties in the last digits (one standard deviation). [a] Jaćimović (2020); [b] De Corte and Simonits (2003); [c] Farina Arboccò et al. (2014); [d] X. Lin and Von Gostomski (2013); n.r. not reported. The energy of 248.96 keV from $^{131}$Ba corresponds the sum of the 246.885 and 249.432 keV gamma energies.

**Table 5**
Results obtained for $Q_0$. There is a comparison between the $Q_0$ values obtained in this work and from the literature applying the Zeta score parameter. Agreement was considered for Zeta below 3.0 (99% confidence interval). The numbers inside parentheses correspond to uncertainties in the last digits (one standard deviation). The references are indicated by a superscript and are described at the bottom of the table.

| Reaction | $Q_0$ | | | | | Zeta Score factor between pairs of $Q_0$ values | | | |
|---|---|---|---|---|---|---|---|---|---|
| | Present Work | Literature (indicated as superscript) | | | | | | | |
| $^{121}$Sb(n.γ)$^{122}$Sb | 28.6(20) | 33.0(12) a, b | | 34.7(7) c | 34.7(46) d | −1.86 a, b | | −2.81 c | −1.23 d |
| $^{123}$Sb(n. γ)$^{124}$Sb | 24.21(94) | 19.9(40) a | 28.8(11) b | 30.5(6) c | 31(56) d | 1.06 a | −3.23b | −5.60 c | −1.18 d |
| $^{130}$Ba(n.γ)$^{131}$Ba | 23.76(92) | 21.3(3) a | 24.8 b | | 19.54(317) d | 2.54 a | | | 1.28 d |

The numbers inside parentheses are the uncertainties in the last digits (one standard deviation). [a] Jaćimović (2020); [b] De Corte and Simonits (2003); [c] Farina Arboccò et al. (2014); [d] Mughabghab (Trkov, 2002).

The $Q_0$ factors from this work for the $^{121}$Sb(n,γ)$^{122}$Sb, $^{123}$Sb (n,γ)$^{124}$Sb and $^{130}$Ba(n,γ)$^{131}$Ba reactions agree with the values of the Jaćimović (2020). The $Q_0$ factor for $^{122}$Sb agrees with De Corte and Simonits (2003) and Mughabghab (Trkov, 2002), and agrees marginally with Farina Arboccò et al. (2014).

The $Q_0$ factor from the present work for $^{124}$Sb agrees with the Mughabghab (Trkov, 2002) and it does not agree with the $Q_0$ values of De Corte and Simonits (2003) and Farina Arboccò et al. (2014). The $Q_0$ factor obtained for $^{131}$Ba in this work also agrees with Mughabghab (Trkov, 2002). These latter values are theoretical, calculated from tabulated thermal cross section and resonance integral values.

The total uncertainties in $k_0$ and $Q_0$ factors from the present work and the corresponding correlation matrix for the $^{121}$Sb(n,γ) $^{122}$Sb, $^{123}$Sb (n,γ) $^{124}$Sb and $^{130}$Ba(n,γ) $^{131}$Ba reactions are shown in Tables 6 and 7, respectively. This information may be required when using the present results for other applications. The correlation factor between the $k_0$ values is positive and the correlation factors between pairs of $Q_0$ values are also positive. The correlation between $k_0$ and $Q_0$ values are negative. In this case, the comparator component appears in the denominator for $k_0$ and in the numerator for $Q_0$. Therefore, the rise in this component

**Table 6**
$k_0$ and $Q_0$ factors and the corresponding Correlation Matrix for $^{121}$Sb(n,γ) $^{122}$Sb and $^{121}$Sb(n,γ) $^{122}$Sb reactions. The numbers inside parentheses correspond to uncertainties in the last digits (one standard deviation).

| Reaction | Parameter | Energy (keV) | Value | Correlation Matrix (x 1000) | | | | | | | | |
|---|---|---|---|---|---|---|---|---|---|---|---|---|
| $^{121}$Sb(n. γ) $^{122}$Sb | $k_0$ | 564.2 | 4.45(7) × $10^{-2}$ | **1000** | | | | | | | | |
| | | 692.7 | 2.34(3) × $10^{-3}$ | **798** | **1000** | | | | | | | |
| | $Q_0$ | Average | 28.6(20) | **−304** | **−269** | **1000** | | | | | | |
| $^{123}$Sb(n. γ) $^{124}$Sb | $k_0$ | 602.73 | 3.02(4) × $10^{-2}$ | **870** | **806** | **−304** | **1000** | | | | | |
| | | 645.85 | 2.25(3) × $10^{-3}$ | **752** | **875** | **−252** | **777** | **1000** | | | | |
| | | 722.78 | 3.26(5) × $10^{-3}$ | **783** | **877** | **−267** | **803** | **902** | **1000** | | | |
| | | 1690.97 | 1.43(2) × $10^{-2}$ | **841** | **847** | **−305** | **849** | **838** | **854** | **1000** | | |
| | | 2090.95 | 1.65(2) × $10^{-3}$ | **629** | **833** | **−208** | **664** | **898** | **874** | **763** | **1000** | |
| | $Q_0$ | Average | 24.21(94) | **−299** | **−265** | **510** | **−300** | **−249** | **−263** | **−301** | **−206** | **1000** |

**Table 7**
$k_0$ and $Q_0$ factors and the corresponding Correlation Matrix for $^{130}$Ba(n,γ) $^{131}$Ba reaction. The numbers inside parentheses correspond to uncertainties in the last digits (one standard deviation).

| Reaction | Parameter | Energy (keV) | Value | Correlation Matrix (x 1000) | | | | | | | | | | | |
|---|---|---|---|---|---|---|---|---|---|---|---|---|---|---|---|
| $^{130}$Ba(n. γ) $^{131}$Ba | $k_0$ | 123.81 | 3.56(13) × $10^{-5}$ | **1000** | | | | | | | | | | | |
| | | 133.61 | 2.74(12) × $10^{-6}$ | **737** | **1000** | | | | | | | | | | |
| | | 216.08 | 2.61(4) × $10^{-5}$ | **994** | **805** | **1000** | | | | | | | | | |
| | | 239.63 | 4.43(14) × $10^{-6}$ | **677** | **996** | **751** | **1000** | | | | | | | | |
| | | 248.96 | 3.89(49) × $10^{-6}$ | **386** | **563** | **428** | **565** | **1000** | | | | | | | |
| | | 249.43 | 4.04(28) × $10^{-6}$ | **386** | **563** | **428** | **565** | **1000** | **1000** | | | | | | |
| | | 373.25 | 1.94(3) × $10^{-5}$ | **921** | **939** | **956** | **907** | **514** | **514** | **1000** | | | | | |
| | | 404.05 | 1.90(18) × $10^{-6}$ | **409** | **617** | **456** | **621** | **997** | **997** | **557** | **1000** | | | | |
| | | 486.52 | 3.25(15) × $10^{-6}$ | **679** | **996** | **753** | **1000** | **565** | **565** | **909** | **621** | **1000** | | | |
| | | 496.33 | 6.46(8) × $10^{-5}$ | **995** | **784** | **996** | **729** | **415** | **415** | **950** | **442** | **732** | **1000** | | |
| | | 620.11 | 2.09(13) × $10^{-6}$ | **636** | **990** | **715** | **999** | **564** | **564** | **884** | **621** | **998** | **692** | **1000** | |
| | | 1047.60 | 1.72(16) × $10^{-6}$ | **613** | **986** | **694** | **997** | **562** | **562** | **870** | **620** | **996** | **671** | **1000** | **1000** |
| | $Q_0$ | Average | 23.76 (92) | **−62** | **−21** | **−60** | **−14** | **86** | **86** | **−35** | **82** | **−13** | **−50** | **−9** | **−7** | **1000** |

tends to decrease $k_0$ and increase the $Q_0$ value.

## 4. Conclusions

The $k_0$ and $Q_0$ factors were measured for $^{121}$Sb, $^{123}$Sb and $^{130}$Ba targets. The irradiations were performed near the IEA-R1 research reactor core at a location where the parameter $\alpha$ is very close to zero, corresponding to an almost ideal epithermal neutron field. Detailed comparison has been performed with the literature.

## Declaration of competing interest

The authors declare that they have no known competing financial interests or personal relationships that could have appeared to influence the work reported in this paper.

## Acknowledgments

The authors are indebted to the National Nuclear Energy Commission (CNEN, Brazil) for sponsoring the postdoctoral fellowship of one of the authors (contract number 01342.002314/2019–57).

## References

Barros, L.F., 2018. Determinação de $k_0$ e $Q_0$ para as reações $^{74}$Se(n, γ) $^{75}$Se, $^{113}$In(n, γ) $^{114m}$In, $^{186}$W(n, γ) $^{187}$W e $^{191}$Ir(n, γ) $^{192}$Ir. PhD Thesis. Universidade de São Paulo, Portuguese. https://doi.org/10.11606/T.85.2018.tde-21092018-143710.

Barros, L.F., Ribeiro, R.V., Dias, M.S., Moralles, M., Semmler, R., Yamazaki, I.M., Koskinas, M.F., 2019. Determination of $k_0$ and $Q_0$ for $^{74}$Se, $^{113}$In, $^{186}$W and $^{191}$Ir targets applying covariance analysis. Appl. Radiat. Isot. 154, 108846. https://doi.org/10.1016/j.apradiso.2019.108846.

Chilian, C., Sneyers, L., Vermaercke, P., Kennedy, G., 2014. Measurement of $k_0$ and $Q_0$ values for iridium isotopes. J. Radioanal. Nucl. Chem. 300, 609–613.

De Corte, F., 1987. The $k_0$-Standardization Method: a Move to the Optimization of Neutron Activation Analysis. Rijksuniversiteit Gent. PhD Thesis.

De Corte, F., Simonits, A., 2003. Recommended nuclear data for use in the $k_0$ standardization of neutron activation analysis. Atomic Data Nucl. Data Tables 85, 47–67.

De Corte, 2010. Towards na international authoritative system for coordination and management of a unique recommended $k_0$-NAA database. Nucl. Instrum. Methods Phys. Res., Sect. A 622, 373–376.

Dias, M.S., Alpino, V., 2001. 1– User Manual. Internal Report. Nuclear Metrology Laboratory. IPEN-CNEN/SP, São Paulo, Brazil.

Dias, M.S., Cardoso, V., Vanin, V.R., Koskinas, M.F., 2004. Combination of nonlinear function and mixing method for fitting HPGe efficiency curve in the 59–2754kev energy range. Appl. Radiat. Isot. 60, 683–687.

Dias, M.S., Moreira, D.S., 2005. LOGFIT V.1– Program for Polynomial Fitting with Covariance. User Manual. Internal Report. Nuclear Metrology Laboratory. IPEN-CNEN/SP, São Paulo, Brazil.

Dias, M.S., Cardoso, V., Koskinas, M.F., Yamazaki, I.M., 2010. Determination of the neutron spectrum shape parameter $\alpha$ in $k_0$ NAA methodology using covariance analysis. Appl. Radiat. Isot. 68, 592–595.

Dias, M.S., Cardoso, V., Koskinas, M.F., Yamazaki, I.M., Semmler, R., Moralles, M., Zahn, G.S., Genezini, F.A., de Menezes, M.O., Figueiredo, A.M.G., 2011. Measurements of $k_0$ and $Q_0$ values for $^{64}$Zn(n,γ)$^{65}$Zn and $^{68}$Zn(n,γ)$^{69m}$Zn reactions with covariance analysis. Appl. Radiat. Isot. 69, 960–964.

Dias, M.S., Semmler, R., Moreira, D.S., de Menezes, M.O., Barros, L.F., Ribeiro, R.V., Koskinas, M.F., 2018. SUMCOR: cascade summing correction for volumetric sources applying MCNP6. Appl. Radiat. Isot. 134, 205–211.

Farina Arboccò, F., Vermaercke, P., Smits, K., Sneyers, L., Strijckmans, K., 2014. Experimental determination of $k_0$, $Q_0$ factors, effective resonance energies and neutron cross-sections for 37 isotopes of interest in NAA. J. Radioanal. Nucl. Chem. 302, 655–672.

Farina Arboccò, F., 2017. Experimental Determination and Re-evaluation of Nuclear Data for the Parametric and $k_0$- Standardization of Neutron Activation Analysis. Ghent University, Belgium. http://hdl.handle.net/1854/LU-8538508.

Firestone, R.B., Trkov, A., 2005. First research coordination Meeting on reference Database for Neutron Activation Analysis – Summary Report. Vienna, Austria. https://doi.org/10.2172/925522.

Firestone, R.B., Kellett, M.A., 2008. Second research coordination Meeting on reference Database for Neutron Activation Analysis – Summary Report. Berkeley, CA. https://doi.org/10.2172/941672.

Hypermet, 2008. Institute of Isotopes, Budapest. www.iki.kfki.hu/nuclear/hypc/index_en.shtml.

ISO 13528, 2015. Statistical methods for use in proficiency testing by interlaboratory comparison. https://www.iso.org/obp/ui/#iso:std:iso:13528:ed-2:v2:en.

Jaćimović, R., De Corte, F., Kennedy, G., Vermaercke, P., Revay, Z., 2014. The 2012 recommended $k_0$ database. J. Radioanal. Nucl. Chem. 300, 589–592.

Jaćimović, R., August 2020. $k_0$ Database [WWW Document]. http://www.kayzero.com/k0naa/k0naaorg/Nuclear_Data_SC/Entries/2020/8/24_Update_of_k0-database_I-128.html, 5 jan 2021.

Kellett, M.A., 2009. Reference Database for Neutron Activation Analysis. IAEA Nuclear Data Section Co-ordinated Research Project [WWW Document]. https://www-nds.iaea.org/naa/index.htmlx, 5 may 2021.

Li, X., Van Sluijs, R., Kennedy, G., 2021. Measurement of $k_0$ values for europium, lutetium and iridium at FRM II with a very well thermalized neutron spectrum. J. Radioanal. Nucl. Chem. 327, 533–542. https://doi.org/10.1007/s10967-020-07500-2.

Lin, X., Henkelmann, R., Alber, D., 2007. Is there something wrong in the barium determination by $k_0$-INAA? J. Radioanal. Nucl. Chem. 271, 71–76.

Lin, X., Von Gostomski, C.L., 2013. Determination of the $k_0$-values for $^{75}$Se, $^{110m}$Ag, $^{115}$Cd–$^{115m}$In, $^{131}$Ba, and $^{153}$Sm by irradiation in highly thermalized neutron flux. J. Radioanal. Nucl. Chem. 295, 1921–1925.

Semkow, T.M., Mehmood, G., Parekh, P.P., Virgil, M., 1990. Coincidence summing in gamma-ray spectroscopy. Nucl. Instrum. Methods Phys. Res. Sect. A Accel. Spectrom. Detect. Assoc. Equip. 290, 437–444.

Stopic, A., Bennett, J.W., 2014. Measurement of $k_0$ values for caesium and iridium. J. Radioanal. Nucl. Chem. 300, 593–597.

Trkov, A., 2016. MATSSF- Material Attenuation Self Shielding Factor [WWW Document]. www-nds.iaea.org/naa/matssf/. URL www-nds.iaea.org/naa/matssf. (Accessed September 2020).

Trkov, A., Kaiba, T., Žerovnik, G., Revay, Z., Firestone, R., Jaćimovic, R., Radulovic, V., 2015. Supplementary Data for Neutron Activation Analysis. INDC (NDC)-0693.

Trkov, A., 2002. Validation of Thermal Cross Sections and Resonance Integrals of SG-23 Evaluated Nuclear Data Library. IAEA, Vienna.